Porous Nylon-6 Fibers via a Novel Salt-Induced Electrospinning Method

Amit Gupta,[†,‡] Carl D. Saquing,[‡] Mehdi Afshari,[†] Alan E. Tonelli,[†] Saad A. Khan,*[,‡] and Richard Kotek*[,†]

Fiber and Polymer Science, College of Textiles, North Carolina State University, Raleigh, North Carolina 27695-830, and Department of Chemical & Biomolecular Engineering, North Carolina State University, Raleigh, North Carolina 27695-7905

Received August 24, 2008; Revised Manuscript Received November 29, 2008

ABSTRACT: Porous nylon-6 fibers are obtained from Lewis acid−base complexation of gallium trichloride ($GaCl_3$) and nylon-6 using electrospinning followed by $GaCl_3$ removal. DSC and FTIR results reveal that the electrospun fibers, prior to $GaCl_3$ removal, are amorphous with no hydrogen bonds present between nylon-6 chains. $GaCl_3$ being a Lewis acid interacts with the Lewis base sites (C═O groups) on the nylon-6 chains, thereby preventing the chains to crystallize via intermolecular hydrogen bonding. Subsequent removal of $GaCl_3$ from the as-spun fibers by soaking the electrospun web in water for 24 h leads to the formation of pores throughout the fibers. While the average fiber diameter remains effectively the same after salt removal, the average surface area increases by more than a factor of 6 for the regenerated fibers. The dual use of a metal salt (Lewis acid) to (a) facilitate fiber formation by temporary removal of polymer interchain interactions and (b) act as a porogen provides a facile approach to obtain porous fibers via electrospinning.

Introduction

Conventional fiber spinning techniques such as melt, wet, and dry spinning can produce fibers with diameters down to the micron range. If the fiber diameter is reduced from micrometers to nanometers, very large surface-area-to-volume ratios and flexibility in surface functionalities can be obtained. These unique qualities make nanofibers an interesting candidate for many important applications.[1] Electrospinning is a process for producing fibers with diameters ranging from 50 to 800 nm from an electrostatically driven jet of polymer solution or melt.[2] In this process a high electrical potential (typically 10−30 kV) is applied to a polymer solution or melt in a syringe. The electric field thus generated produces a driving force, and the polymer jet is ejected from the tip of the cone. The jet begins to whip or splits into bundles of smaller fibers which are collected on a grounded collector. This technique can be used for producing uniform fibers with novel compositions and morphologies such as hollow, core−sheath, and porous fibers.[3,4]

Two approaches have generally been undertaken in the area of electrospinning: examining the effects of process/material parameters and development of new functionalities. From the materials/process standpoint, several factors can influence the transformation of polymer solutions into fibers through electrospinning. These parameters include (a) intrinsic properties of the solution such as rheology, conductivity, surface tension, and polymer molecular weight and concentration and (b) operational conditions such as electric field strength, solution flow rate, nozzle diameter, spinneret−collector distance, and motion of the collector.[5−13] However, many of these parameters are interdependent of each other; for example, solution rheology is a function of both polymer molecular weight and solution concentration while electric field strength, solution flow rate, and nozzle diameter are inter-related. As such, the focus of many studies has been on examining ways to control diameter of the resulting nanofibers.

On the other hand, functionalization of nanofibers expands its scope for a wide range of applications such as membranes, filters, biological sensors, scaffolds, transport media, lightweight reinforcement, and coatings.[1,14−21] Many of these applications could be greatly enhanced by increasing the surface area and porosity of the fibers. As such, several groups have attempted production of porous fibers using different approaches. Researchers have reported that by using a highly volatile solvent in the electrospinning process porous fibers or fibers with unusual surface structures could be obtained.[22−24] Recently, Dayal and co-workers[25] have spun fibers from amorphous polymer solutions of poly(methyl methacrylate)/methylene chloride and poly(styrene)/tetrahydrofuran and generated nanopores via solvent evaporation. From their work they found that porous fiber formation is favored if the polymer/solvent system is partially miscible, showing a UCST behavior at the electrospinning temperature. Electrospinning of sol−gel solutions of inorganic materials with surfactants can also produce porous fibers.[26] McCann and co-workers showed that by using a coaxial spinneret with miscible solvents and immiscible polymers highly porous fibers could be obtained by selective dissolution for polymer fibers and calcinations for composite fibers.[3] They also produced porous polystyrene, polyacrylonitrile, and poly(vinylidene fluoride) fibers by immersing the collector in a bath of liquid nitrogen followed by drying in vacuum.[27] The porous fibers were obtained through thermally induced phase separation between the solvent-rich and solvent-poor regions in the fiber during electrospinning.

Several research groups have also produced porous fibers by electrospinning polymer blends, followed by selective removal of one component.[3,23,28] For example, Bognitzki and co-workers[29] synthesized porous fibers of poly(lactic acid) (PLA) and polyvinylpyrrolidone (PVP) by electrospinning a PLA/PVP blend solution. Zhang et al.[30] used the concept of phase separation with electrospinning to generate polyacrylonitrile (PAN) and poly(ethylene oxide) (PEO) bicomponent fibers (15−50 wt % of PEO in PAN). The nanopores were generated by dissolution of the phase-separated PEO domains in water and the selective removal of the PEO component. However, they found that removal of one component increased the average

* Corresponding authors: phone 919-515-4519, e-mail khan@eos.ncsu.edu (S.A.K.); phone 919-515-6585, e-mail richard_kotek@ncsu.edu (R.K.).
† Fiber and Polymer Science, College of Textiles.
‡ Department of Chemical & Biomolecular Engineering.

10.1021/ma801918c CCC: $40.75
Published on Web 12/23/2008

fiber diameters. Although viable in principle, nanopore generation via this method is time intensive due to the slow solubilization of most polymers, and in some cases complete removal of the unwanted component may not be possible.

Addition of salts into an electrospinning system is another way to control the fiber structure and properties. Mit-uppatham and co-workers[31] added NaCl, LiCl, and $MgCl_2$ to solutions of nylon-6 in formic acid and found that increasing salt concentration increased solution viscosity, conductivity, and fiber diameter. They suggested the increase in fiber diameter to be a result of increasing solution viscosity and mass flow. In general, the addition of salt may increase or decrease the solution viscosity depending on the interactions among salt, polymer, and solvent.[32−36] Phadke et al.[36] investigated the effect of three different salts (LiCl, $ZnCl_2$, and $AlCl_3$) with *N,N*-dimethylformamide (DMF) and polyacrylonitrile (PAN). They found that salt addition had two opposing effects: (i) decrease in DMF solvent power, which caused less expanded polymer coils (i.e., lower viscosity), and (ii) increase in interpolymer chain entanglements via salt-promoted chain association (i.e., higher viscosity). As a result, adding salts increases the viscosity of low-molecular-weight (MW, 50 kDa) PAN solution but decreases the viscosity of high-MW (150 and 250 kDa) PAN solutions. Adding salts into polymer solutions is also a common method to adjust the solution (ionic) conductivity. Different salts such as sodium chloride[37] and triethylbenzylammonium chloride[28] have been added to polymer solutions (e.g., PEO/water[37] and polyurethaneurea/DMF[28]) to increase the ionic conductivity and consequent mass flow that passes through the spinneret nozzle. The increased ionic conductivity also favors formation of bead-free fibers and reduction in fiber diameter.[37]

In this paper we report production of porous fibers via electrospinning from a Lewis acid−base complex of nylon-6 and $GaCl_3$. Initial study by Roberts and Jenekhe has demonstrated that polyamides can undergo complex formation with strong Lewis acids such as $GaCl_3$ by interacting with the Lewis base sites (CO−NH) along the polymer chain.[38] More recently, Kotek and Tonelli in our laboratory have tried to use this approach to obtain high-modulus fibers using conventional fiber drawing techniques.[39] We exploit this concept to show that removal of crystallinity and hydrogen bonding between polyamide chains via salt addition facilitates electrospinning. Subsequent removal of salt from the electrospun fiber of nylon-6/$GaCl_3$ complex using water (regeneration/decomplexation) results in *in situ* generation of nanosized pores. Such an approach in which the salt is used as both a facilitator for electrospinning as well as a porogen has not been reported before and provides an attractive method to obtain porous fibers.

Experimental Section

Material. Nylon-6 pellets (ULTRAMID B40 01) with a viscosity-average molecular weight of 63 000 g/mol were obtained from BASF Corporation (Michigan) and used as received. The viscosity-average molecular weight was calculated from the Mark−Houwink's equation. The constants K and a used for the nylon-6/formic acid system at 25 °C were 22.6×10^{-5} dL/g and 0.82, respectively,[40] and the viscometric measurements were conducted at 25 °C using an Ubbelohde viscometer.

Preparation of Nylon-6/$GaCl_3$ Complex Solutions. A polymer concentration of 5 wt % was used in making the complex solutions (Nylon-6/$GaCl_3$) in nitromethane at around 70 °C. The solution was held under nitrogen for ∼10−12 h, and mechanical stirring was used for dissolving the nylon-6 pellets completely. The viscosity of the solution was found to be 0.3 Pa·s. A 1.1:1 stoichiometric ratio of $GaCl_3$ to amide groups (CO−NH) was used to achieve complete suppression of hydrogen bonding in nylon-6.

Electrospinning. For electrospinning of nylon-6, a variable high-voltage power supply (Glassman high-voltage model FC60R2 with positive polarity) was used to apply voltage of 20 kV. The polymer solution was placed in a 10 mL syringe, to which a capillary tip of 0.4 mm inner diameter was attached. The positive electrode of the high-voltage power supply was connected to the capillary tip. The grounded electrode was connected to a metallic collector wrapped with aluminum foil. The distance between tip to collector and flow rate were maintained at 16 cm and 1 mL/h, respectively.

Morphology of Electrospun Webs. The morphology and diameter of the as-spun and regenerated nylon-6 webs were observed by using scanning electron microscopy (Hitachi S-3200 and FEI XL30 SEM, both operating at an accelerating voltage of 5 kV). The electrospun samples were coated by a K-550X sputter coater with Au/Pd ∼100 Å thick to reduce charging. Transmission electron microscopy (TEM) (FEI Tecnai G^2 Twin and Hitachi HF-2000) was also used to study the structure of composite/as-spun and porous/regenerated fibers placed on 200-mesh Cu grids with an accelerating voltage of 200 kV. A cross section of the regenerated fibers was prepared by ultramicrotomy techniques. A bundle of electrospun fibers was embedded in Spurr's epoxy resin, and then a section was sliced using a diamond edged blade. Ultramicrotomed samples were analyzed by both SEM and TEM techniques.

Thermal Analysis. The melting temperature was measured with a Perkin-Elmer differential scanning calorimeter (DSC 7). Each thermogram was obtained from 25−240 °C at a heating and cooling rate of 20 °C/min. No subambient scans were undertaken as previous work has already examined that and reported the T_g of the nylon-6/gallium chloride complex to be −32 °C,[39] substantially lower than that of of nylon-6. The instrument was calibrated using indium. Approximately 3 mg of sample was used in a nitrogen environment.

FTIR Spectroscopy. Attenuated total reflectance (ATR) spectra were collected on a Nicolet 560 FTIR spectrometer equipped with an Advantage microscope and using liquid nitrogen cooled mercury cadmium telluride (MCT) detector. At least 32 scans were obtained to achieve an adequate signal-to-noise ratio. The spectral resolution was 2 cm^{-1}.

BET Surface Area and Pore Size Analysis. BET surface areas were determined from N_2 adsorption isotherm data collected at 77 K (Autosorb-1-MP, Quantachrome Corp., Boynton Beach, FL). Prior to analysis, adsorbent samples were outgassed for 12 h at 313 K. BET surface areas were determined from 18-point adsorption isotherms that were completed with at least 0.2 g sample in the 0.01−0.3 relative pressure range. A glass rod was used during the analysis to decrease the void volume of the sample holder.

Pore size distributions were determined by conducting N_2 adsorption experiments constructed from 126 data points in the relative pressure range of 10^{-6}−1 using a sample mass of 1.0 g of adsorbent. A glass filler rod was inserted into the sample holder to minimize the void volume in the sample holder during the analysis. Micropore volume, mesopore volume, and pore size distribution were computed from N_2 adsorption isotherm data using the density functional theory (DFT) with the N2_carb1.gai kernel (PC software version 1.51, Quantachrome, Boynton Beach, FL). In addition, the mesopore volume was computed using the Barrett, Joyner, and Halenda (BJH) and DFT methods. The BJH method is commonly used to determine the volume and size distribution of mesopores (2−50 nm) and small macropores, and the DFT method is typically used to estimate the volume and size distribution of micropores (<2 nm) and small mesopores.[41,42]

Results and Discussion

As a primer to electrospinning, complexes of nylon-6 with $GaCl_3$ were prepared at stoichiometric ratios of 1:1 and 1.1:1 ($GaCl_3$:C═O). The spinnability of the complex solution and drawability in the resulting fibers were examined for these compositions using the conventional dry-jet wet spinning technique. Although a ratio of 1:1 was sufficient to completely dissolve nylon-6 in the solution of $GaCl_3$ in nitromethane, improved spinnability was achieved with a ratio of 1.1:1. This was further supported by the fact that continuous fibers could

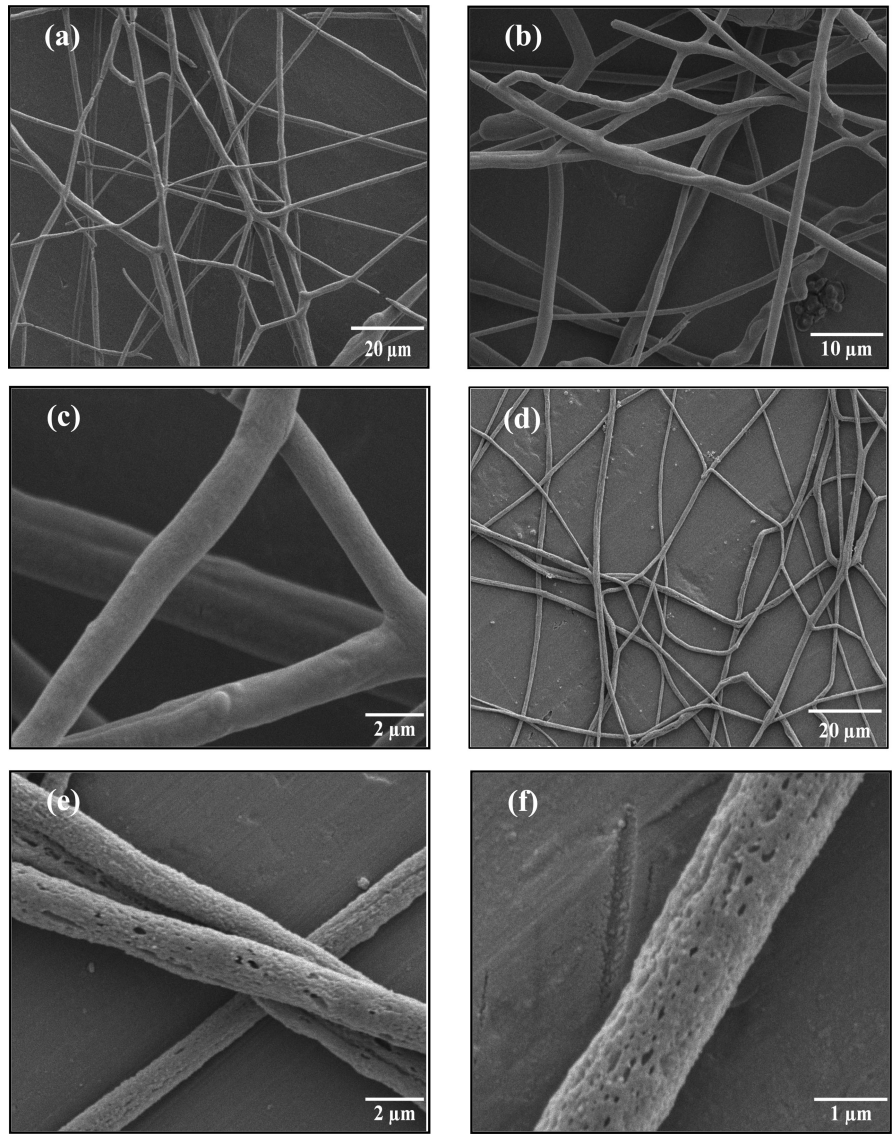

Figure 1. SEM micrographs of as-spun nylon-6 fibers (a−c) and regenerated nylon-6 porous fibers (d−f).

also be spun with enhanced drawability for this sample using a dry-jet wet spinning apparatus. Fibers with diameters ∼250 μm were obtained from the above-mentioned technique. The diameter of fibers obtained with the ratio 1:1 was larger (∼400 μm) compared to that of the 1.1:1 ratio due to reduced drawability. For this reason complex solutions with ratio of 1.1:1 between $GaCl_3$ and C═O were used in the electrospinning process; all subsequent results reported in this study correspond to this composition.

Figure 1 shows SEM micrographs of electrospun nylon-6 fibers containing $GaCl_3$. These *as-spun/nonregenerated* fibers exhibit a smooth surface and uniform diameters along their lengths. The latter aspect is seen more clearly in Figure 1c, which shows the micrograph at a higher magnification. Figure 1d−f shows micrographs of the same fibers upon removal (regeneration) of the $GaCl_3$. We observe that the fiber surfaces have become rough due to the removal of salt. As $GaCl_3$ comes out of the as-spun fibers, it leaves nano- and macropores all along the surface of the fibers. High-resolution SEM images (as shown in Figure 2a,b) of the surface of the regenerated nylon-6 porous fibers allowed us to look closer into these pores, and it appears that the pore structure is also present within the fibers (see inset of Figure 2a). To further support this observation, we looked at the cross section of these fibers in SEM as well as in TEM (as shown in Figure 2c,d). The pores appear to be uniformly distributed throughout the cross section of these fibers. One interesting observation that can be made here is that the as-spun fibers appear to be fused or glued to each other while the regenerated fibers are not. This aspect will be more clearly understood when we discuss the DSC results. Statistical analysis of the fiber diameters was carried out by constructing histograms, from which average diameter and a standard deviation were obtained. Figure 3 shows the fiber diameter distributions of as-spun and regenerated fibers. The average diameter and standard deviation for the as-spun fibers was 1021 ± 398 nm and that for regenerated ones was 1067 ± 299 nm, suggesting that the fiber diameter remained effectively the same after salt removal. The distributions are very broad for both as-spun and regenerated fibers; however, the distribution shifts to lower diameters for regenerated fibers which is evident from the lower standard deviation.

Figure 4a,b shows the TEM images of as-spun fibers and Figure 4c,d for regenerated ones. The images of as-spun fibers are mostly dark (as would be expected for solid homogeneous fibers) with darker spots uniformly distributed throughout the fibers due to the contrast generated by the presence of $GaCl_3$. The edges of the fibers have smooth surface whereas the images of regenerated fibers display white patches uniformly distributed all over their length (these are highlighted by circles). These white patches are due to the pores in the fibers and their sizes

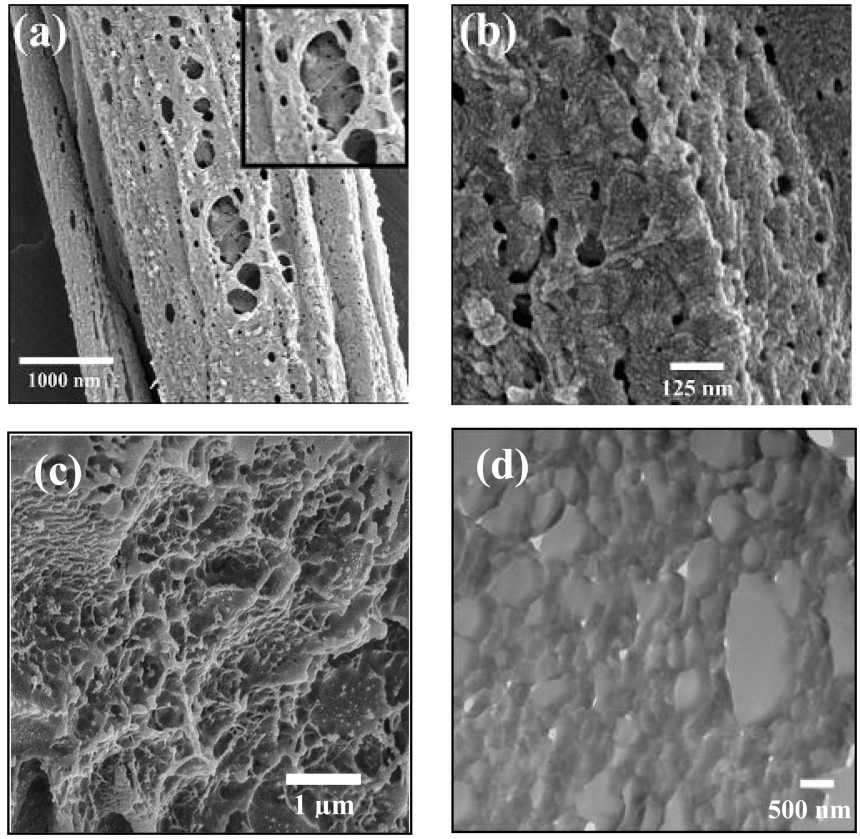

Figure 2. (a, b) High-resolution SEM images of the surface of regenerated nylon-6 porous fibers. (c) SEM image and (d) TEM image of the cross section of regenerated nylon-6 porous fibers (flat regions in the TEM image are from the epoxy resin in which the electrospun fiber bundle was embedded).

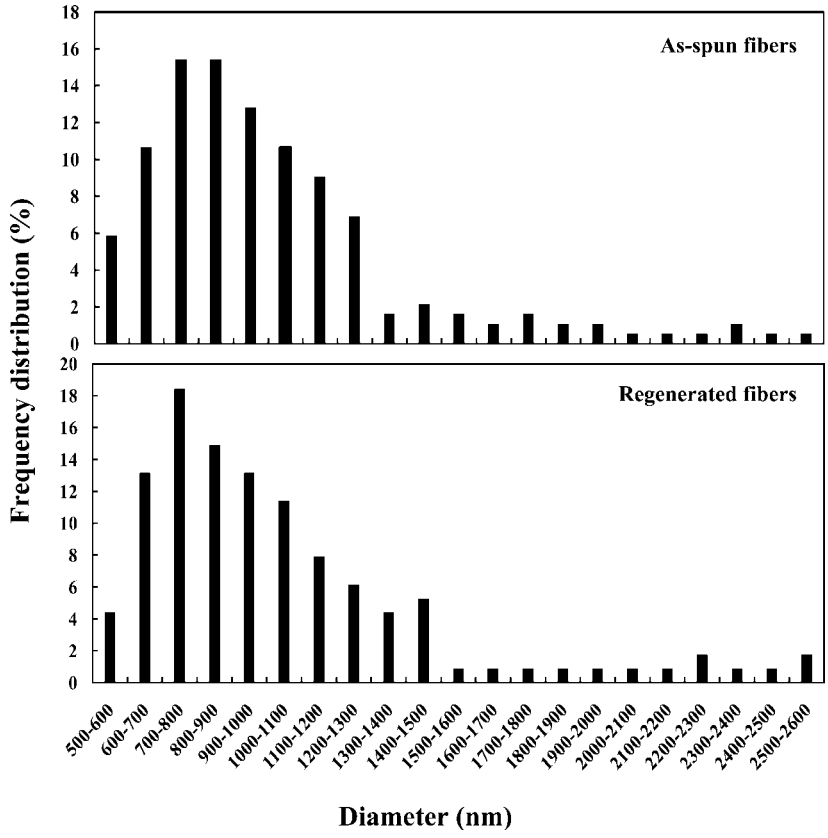

Figure 3. Fiber diameter distributions of as-spun nylon-6 fibers (top) and regenerated nylon-6 porous fibers (below).

match the sizes observed in the respective SEM images. Furthermore, the TEM images for the regenerated fiber (Figure 4d,e) show that, compared to the edges of the as-spun fibers which are smooth and uniform (Figure 4b), the regenerated fiber

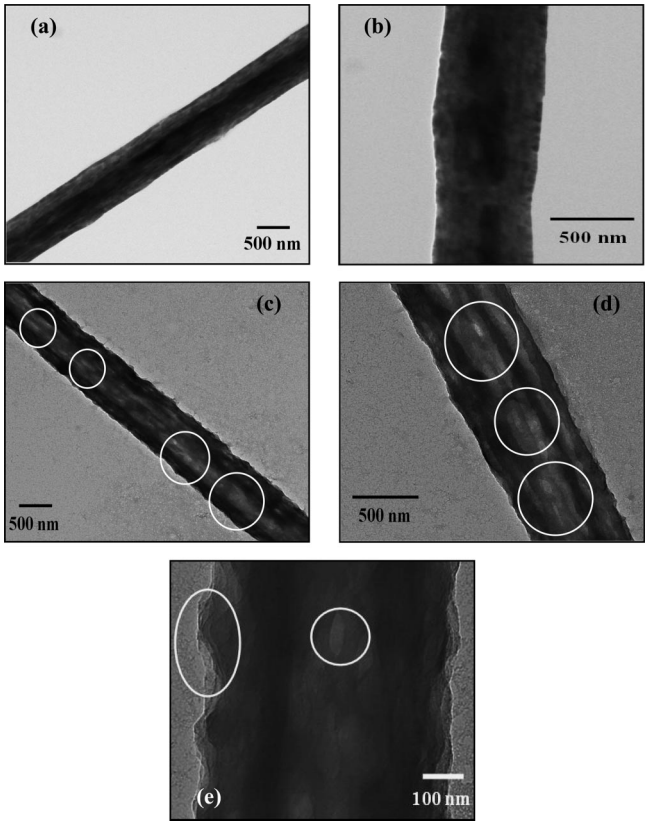

Figure 4. TEM micrographs of as-spun nylon-6 fibers (a, b), regenerated nylon-6 porous fibers (c, d), with circles showing white patches for pores, and regenerated fiber showing differences in edge morphology (e).

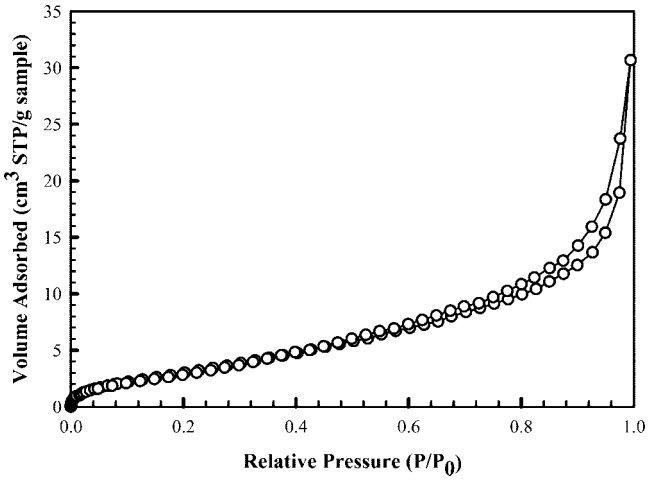

Figure 5. Nitrogen adsorption and desorption isotherm at 77 K of the regenerated electrospun nylon-6 fibers.

has elongated indents and ridges (encircled) as well as highly uneven morphology along the edges. These indicate that morphological modification has taken place in regenerated fibers as a result of salt removal. The results from BET surface area measurements also support these observations. From BET measurements, we find that the average surface area of the as-spun fibers is 1.8 m^2/g, whereas the regenerated electrospun fibers show a surface area of 12 m^2/g, reflecting an increase of at least a factor of 6.

The increased porosity we obtained is better than what some other researchers have reported in the literature. Zhang and co-workers prepared nanoporous ultrahigh specific surface polyacrylonitrile fibers by electrospinning bicomponent fibers from

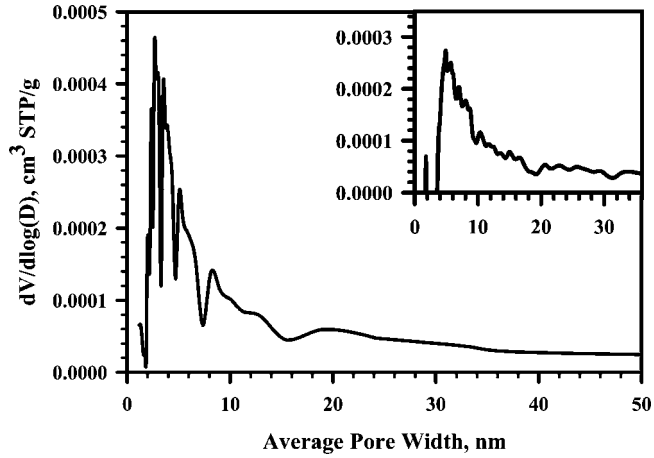

Figure 6. Differential pore volume as a function of pore diameter using the BJH and DFT (inset) methods based on slit/cylindrical pore model for the regenerated electrospun nylon-6 fibers.

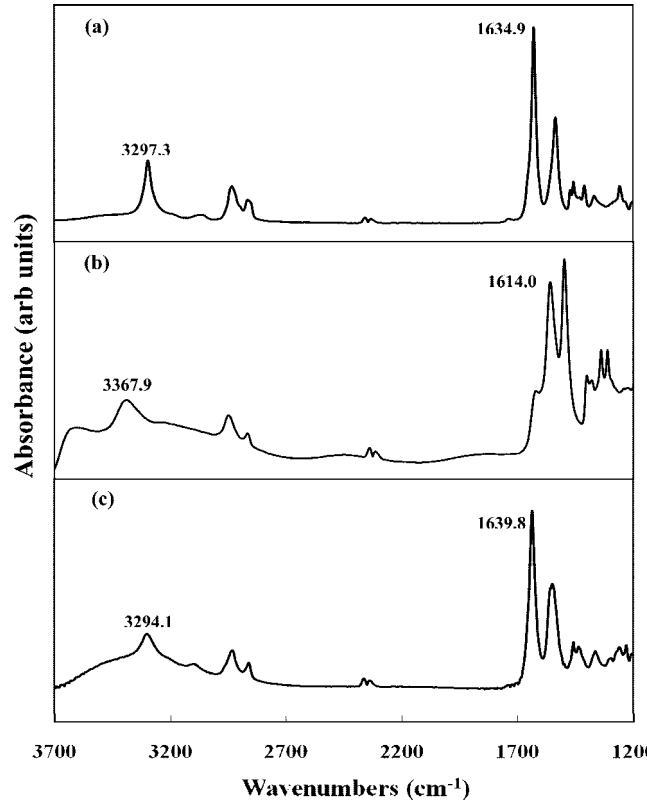

Figure 7. FTIR spectra of (a) reference nylon-6, (b) nylon-6—$GaCl_3$ complex fibers, and (c) regenerated nylon-6 fibers.

solutions of polyacrylonitile and poly(ethylene oxide). Pores were generated by the selective removal of the PEO component, and they found a 2.5-fold increase in surface area compared to the as-spun nonporous fibers.[30] Similarly, Ji and co-workers studied the preparation and characterization of silica nanoparticulate—polyacrylonitrile composite and porous nanofibers. Porous nanofibers were prepared by the selective removal of silica component from the silica/PAN composite fiber, and they found that there was a 20% increase in surface area upon formation of pores.[43]

Figures 5 and 6 present the N_2 physisorption (adsorption/desorption) isotherm and pore size distribution of the regenerated nanofibers, respectively. The isotherm is akin to a type II in accordance to the International Union of Pure and Applied Chemistry (IUPAC) isotherm classification but exhibits a

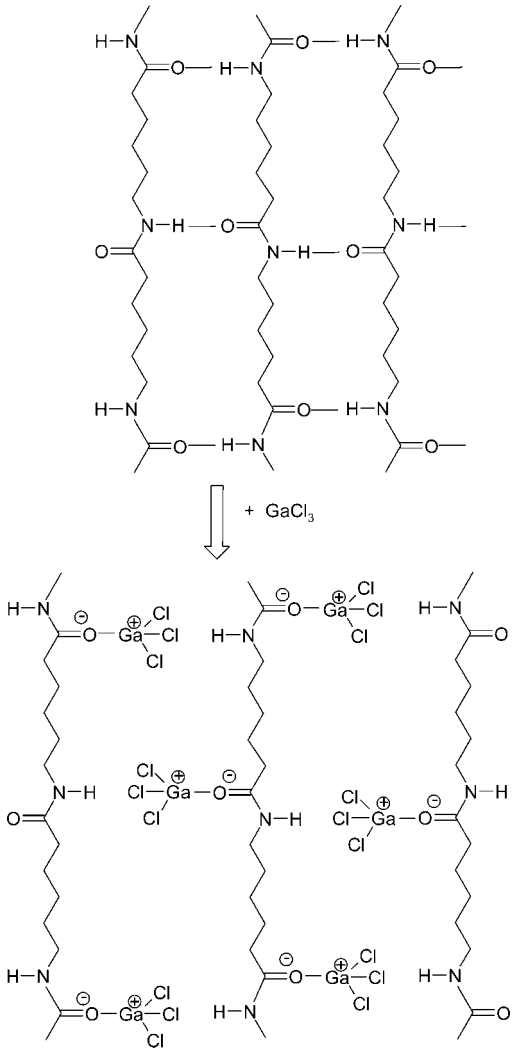

Figure 8. Schematic of reference nylon-6 with intermolecular hydrogen bonds (top) and nylon-6 complexed with $GaCl_3$ (bottom).

hysteresis loop and an inflection point at lower P/P_0 which are associated with the presence of mesopores (2−50 nm pore diameter) and micropores, respectively, in the material.[41,42] The pore size distribution was estimated using both BJH and DFT (inset of Figure 6) methods. The regenerated electrospun nylon-6 fibers mostly contain mesopores with widths in the 3−14 nm pore range according to both the BJH and DFT method. Some micropores (∼1.7 nm) and macropores (>50 nm) were also present as determined from the DFT and BJH methods, respectively. A systematic study on controlling pore size has not been attempted because the focus of this work has been to establish the concept of preparing porous electrospun fibers using this approach. One can however use different solvents, such as methanol and ethanol, or cosolvents to control the removal rate of $GaCl_3$ as a possible route to modulate pore size and pore size distribution.

In order to examine the reaction between $GaCl_3$ and nylon chains, and the role of $GaCl_3$ complexation in facilitating electrospinning, a series of experiments involving FTIR spectroscopy and DSC were performed. Figure 7 shows the infrared spectra of (a) reference nylon-6, (b) nylon-6−$GaCl_3$ complex fiber web, and (c) regenerated/decomplexed nylon-6 fiber web (i.e., after the removal of $GaCl_3$). In Figure 7a, the bands at 3297 and 1635 cm^{-1} have been attributed to N−H and C═O stretching vibrations, respectively. The amide group is potentially a bifunctional electron donor with $2sp^2$ "lone pairs" at the oxygen atom and a $2p_z^2$ "lone pair" at the nitrogen atom

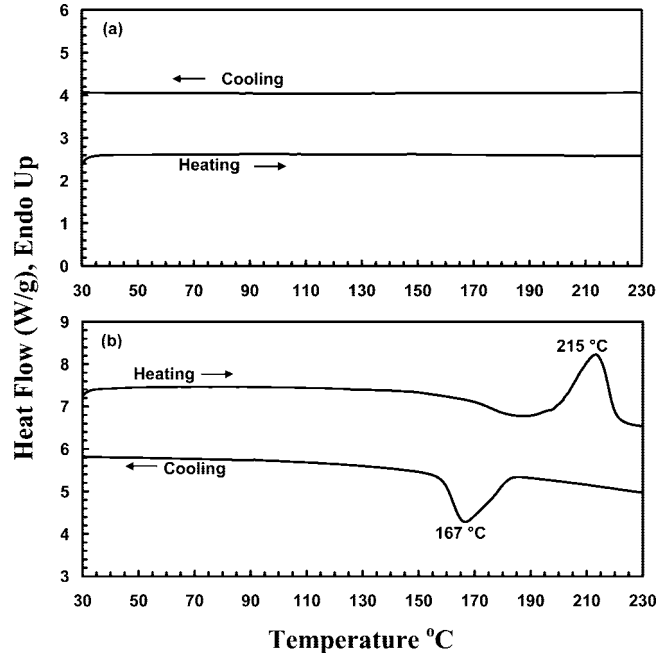

Figure 9. DSC thermogram of nylon-6−$GaCl_3$ as-spun fiber (a) and regenerated nylon-6 fiber (b).

and therefore has two possible electron-donating sites to coordinate with the Ga^{3+} cation. Overlap of $2p_z$ orbitals of the oxygen, carbon, and nitrogen atoms in the planar amide group would reduce the electron density on the nitrogen atom and favor the coordination of the metal ion with the carbonyl oxygen atom. Ga^{3+} metal coordination with the C═O groups in the nylon breaks the intermolecular hydrogen bonds between nylon-6 chains which is schematically shown in Figure 8.[38,44]

Since $GaCl_3$ forms a complex with the C═O group, the N−H bond becomes free. This causes the N−H vibrational band to shift to a higher frequency (red shift from 3297 to 3367 cm^{-1}), while the C═O vibrational band shifts to lower frequency (blue shift from 1635 to 1614 cm^{-1}) due to a reduction in bond order as a result of complexation. This change can be seen in the spectrum of nylon-6−$GaCl_3$ complex fiber web in Figure 7b. Decomplexed nylon-6 fiber web was obtained by soaking the as-spun web in water for at least 24 h although most of the salt is removed within the first few minutes.[44] Water, being a stronger Lewis base than nylon, helps in removing the salt from within the polymer matrix. Other solvents like methanol, ethanol, or isopropanol can also be used, but they may take a much longer time for achieving complete regeneration. From Figure 7c, it can be seen that the infrared spectra of regenerated nylon-6 films and reference nylon-6 films are essentially the same, suggesting that complete removal of the Lewis acid has taken place from the complexed sample.

Differential scanning calorimetry was employed to study the melting and crystallization behaviors of the as-spun and regenerated fiber webs. Figure 9a shows the DSC scan of nylon-6−$GaCl_3$ complexed electrospun fibers. We observe no melting or crystallization peaks during heating or cooling, respectively, of the sample, suggesting that the complex has a completely amorphous morphology. This is due to the fact that for the salt complexes with nylon the C═O groups in the polymer matrix are shielded by the huge and bulky $GaCl_3$ molecules, thereby preventing the chains to crystallize via intermolecular hydrogen bonding (cf. Figure 8). Because of this reason, the as-spun, complexed fibers are sticky and appear glued or fused to each other in the SEM micrographs shown in Figure 1a−c. Figure 9b shows heating and cooling scans for the regenerated nylon-6 electrospun fibers; we can clearly observe the respective melting

and crystallization peaks characteristic of nylon-6 due to the regeneration of the hydrogen bonds between the polyamide chains. The measured melting and crystallization temperatures for the regenerated fibers are ~215 and ~167 °C, respectively, which are similar to the melting and crystallization temperatures of nylon-6 pellets used in this study. This result taken together with the comparable FTIR spectra of the as-spun and regenerated fibers indicates that the introduction and removal of $GaCl_3$ is a reversible process and does not change the final properties of the nylon.

Conclusions

This study demonstrates a two-step approach for producing porous fibers of nylon-6. In the first step, electrospun fibers are obtained from a 5 wt % Lewis acid−base complex solution of nylon-6 and $GaCl_3$ in nitromethane. Subsequent removal of the $GaCl_3$ salt through soaking in water leads to pore formation both within and on the surface of the fibers, as evidenced from SEM and TEM images. Quantitave analysis from BET surface area measurements reveal that the average surface area of the as-spun fibers is 1.8 m^2/g, whereas that of the regenerated (salt removed) electrospun fibers is 12 m^2/g, reflecting an increase of at least a factor of 6. Further, the fiber diameter remains unchanged upon salt removal. These results taken together suggest that Lewis acid−base complexation can be used as an effective method for producing porous nylon fibers and can possibly be extended to other polymers to prepare porous and nanostructured fibers for different applications.

Acknowledgment. The authors gratefully acknowledge the financial help of the National Textile Center and NSF-STC (CHE-9876674) for partial support of this work. They thank Prof. Detlef Knappe of the Dept. of Civil, Construction and Environmental Engineering, NCSU, for assistance and advice with the BET and pore size measurement and Mr. Roberto Garcia of the Analytical Instrumentation Facility (NCSU) for helping in preparing the cross section of the regenerated nylon-6 porous fibers.

References and Notes

(1) Huang, A. Z.; Zhang, Y. Z.; Kotaki, M.; Ramakrishna, S. *Compos. Sci. Technol.* **2003**, *63*, 2223–2253.
(2) Pedicini, A.; Farris, R. J. *J. Polym. Sci., Part B: Polym. Phys.* **2004**, *42*, 752–757.
(3) McCann, J. T.; Li, D.; Xia, Y. *J. Mater. Chem.* **2005**, *15*, 735–738.
(4) Loscertales, I. G.; Barrero, A.; Marquez, M.; Spretz, R.; Velarde-Ortiz, R.; Larsen, G. *J. Am. Chem. Soc.* **2004**, *126*, 5376–5377.
(5) Reneker, D. H.; Chun, I. *Nanotechnology* **1996**, *7*, 216–223.
(6) Fong, H.; Chun, I.; Reneker, D. H. *Polymer* **1999**, *40*, 4585–4592.
(7) Shenoy, S. L.; Bates, W. D.; Frisch, H. L.; Wnek, G. E. *Polymer* **2005**, *46*, 3372–3384.
(8) Gupta, P.; Elkins, C.; Long, T. E.; Wilkes, G. L. *Polymer* **2005**, *46*, 4799–4810.
(9) Ferry, J. D. *Viscoelastic Properties of Polymers*, 2nd ed.; Wiley Interscience: New York, 1980; p 641.
(10) McKee, M. G.; Wilkes, G. L.; Colby, R. H.; Long, T. E. *Macromolecules* **2004**, *37*, 1760–1767.
(11) Demir, M. M.; Yilgor, I.; Yilgor, E.; Erman, B. *Polymer* **2002**, *43*, 3303–3309.
(12) Lee, K. H.; Kim, H. Y.; La, Y. M.; Lee, D. R.; Sung, N. H. *J. Polym. Sci., Part B: Polym. Phys.* **2002**, *40*, 2259–2268.
(13) Liu, H.; Hsieh, Y.-L. *J. Polym. Sci., Part B: Polym. Phys.* **2002**, *40*, 2119–2129.
(14) Kim, T. G.; Park, T. G. *Biotechnol. Prog.* **2006**, *22*, 1108–1113.
(15) Hussain, M. M.; Ramkumar, S. S. *Indian J. Fibre Text. Res.* **2006**, *31*, 41–51.
(16) Huang, Z. M.; Zhang, Y.; Ramakrishna, S. *J. Polym. Sci., Part B: Polym. Phys.* **2005**, *43*, 2852–2861.
(17) Liang, D.; Hsiao, B. S.; Chu, B. *Adv. Drug Delivery Rev.* **2007**, *59*, 1392–1412.
(18) Burger, C.; Chu, B. *Colloids Surf., B* **2007**, *56*, 134–141.
(19) Chu, B.; Liang, D.; Hadjiargyrou, M.; Hsiao, B. S. *J. Phys: Condens. Matter* **2006**, *18*, S2513−S2525.
(20) Burger, C.; Hsiao, B. S.; Chu, B. *Annu. Rev. Mater. Res.* **2006**, *36*, 333–368.
(21) Chiu, J. B.; Luu, Y. K.; Fang, D.; Hsiao, B. S.; Chu, B.; Hadjiargyrou, M. *J. Biomed. Nanotechnol.* **2005**, *1*, 115–132.
(22) Megelski, S.; Stephens, J. S.; Chase, B. D.; Rabolt, J. F. *Macromolecules* **2002**, *35*, 8456–8466.
(23) Bognitzki, M.; Czado, W.; Frese, T.; Schaper, A.; Hellwig, M.; Steinhart, M.; Greiner, A.; Wendorff, J. H. *Adv. Mater.* **2001**, *13*, 70–73.
(24) Casper, C. L.; Stephens, J. S.; Tassi, N. G.; Chase, D. B.; Rabolt, J. F. *Macromolecules* **2004**, *37*, 573–578.
(25) Dayal, P.; Liu, J.; Kumar, S.; Kyu, T. *Macromolecules* **2007**, *40*, 7689–7694.
(26) Madhugiri, S.; Zhou, W.; Ferraris, J. P.; Balkus, K. J. *Microporous Mesoporous Mater.* **2003**, *63*, 75–84.
(27) McCann, J. T.; Marquez, M.; Xia, Y. *J. Am. Chem. Soc.* **2006**, *128*, 1436–1437.
(28) Li, D.; Xia, Y. *Adv. Mater.* **2004**, *16*, 1151–1170.
(29) Bognitzki, M.; Frese, T.; Steinhart, M.; Greiner, A.; Schaper, A.; Hellwig, M.; Wendorff, J. H. *Polym. Eng. Sci.* **2001**, *41*, 982–989.
(30) Zhang, L.; Hsieh, Y. L. *Nanotechnology* **2006**, *17*, 4416–4423.
(31) Mit-uppatham, C.; Nithianakul, M.; Supaphol, P. *Macromol. Chem. Phys.* **2004**, *205*, 22327–2338.
(32) Zhang, L. H.; Zhang, D.; Jiang, B., T. *Chem. Eng. Technol.* **2006**, *29*, 395–400.
(33) Bajaj, P.; Bahrami, S. H.; Sen, K.; Sreekumar, T. V. *J. Appl. Polym. Sci.* **1999**, *74*, 567–582.
(34) Cho, Y. W.; An, S. W.; Song, S. C. *Macromol. Chem. Phys.* **2006**, *207*, 412–418.
(35) Curti, E.; Campana-Filho, S. P. *J. Macromol. Sci., Part A: Pure Appl. Chem.* **2006**, *43*, 555–572.
(36) Phadke, M. A.; Musale, D. A.; Kulkarine, S. S.; Karode, S. K. *J. Polym. Sci., Polym. Phys.* **2005**, *43*, 2061–2073.
(37) Choi, J. J.; Kim, Y. M.; Lee, J. S.; Cho, K. Y.; Jung, H. Y.; Park, J. K.; Park, I. S.; Sung, Y. E. *Solid State Ionics* **2005**, *176*, 3031–3034.
(38) Roberts, M. F.; Jenekhe, S. A. *Macromolecules* **1991**, *24*, 3142–3146.
(39) Afshari, M.; Gupta, A.; Jung, D.; Kotek, R.; Tonelli, A. E.; Vasanthan, N. *Polymer* **2008**, *49*, 1297–1304.
(40) Bandrup, J.; Immergut, E. H. *Polymer Handbook*; Wiley Interscience: New York, 1975.
(41) Olivier, J. P. *Carbons* **1998**, *36*, 1469–1472.
(42) Sing, K. S. W.; Everett, D. H.; Haul, R. A. W.; Moscou, L.; Pierotti, R. A.; Roquerol, J.; Siemienewska, T. *Pure Appl. Chem.* **1985**, *57*, 603–619.
(43) Ji, L.; Saquing, C. D.; Khan, S. A.; Zhang, X. *Nanotechnology* **2008**, *9*, 085605/1−085605/9.
(44) Vasanthan, N.; Kotek, R.; Jung, D.; Shin, D.; Tonelli, A. E.; Salem, D. R. *Polymer* **2004**, *45*, 4077–4085.

MA801918C